JASN-2017-08-0828-R2

Mechanisms of Crystalloid *versus* Colloid Osmosis across the Peritoneal Membrane

Johann Morelle, Amadou Sow, Charles-André Fustin, Catherine Fillée, Elvia Garcia-Lopez, Bengt Lindholm, Eric Goffin, Frederic Vandemaele, Bengt Rippe, Carl M. Öberg*, and Olivier Devuyst*

Supplementary material

TABLE OF CONTENT

DETAILED MATERIAL AND METHODS

Animals. Gender-matched *Aqp1* mouse littermates generated as previously described[1], aged 8–12 weeks, were used to assess the influence of the water channel AQP1. All animals had access to standard diet and tap water *ad libitum*. The experiments were conducted in accordance with the National Research Council Guide for the Care and Use of Laboratory Animals and the Animal Ethics Committee of the UCL Medical School.

Peritoneal transport studies. Transport across the mouse peritoneum was investigated using a modified peritoneal equilibration test with different PD solutions (Baxter Healthcare, Belgium) (Table 1), as described previously[2-6]. The combined glucose-icodextrin PD solutions were prepared by Baxter on laboratory scale using the same raw materials as the current glucose and icodextrin PD solutions. These PD solutions were filtered through a 0.2 µm filter, filled into bags, overpouched, heat sterilized, and their final electrolyte composition was verified. Although no endotoxin screening was performed, the lack of impact of these solutions on solute transport - as compared with commercial solutions – rules out any significant inflammation. Briefly, following anesthesia with ketamine (100 mg/kg SC, Merial, Brussels, Belgium) and xylazine (10 mg/kg subcutaneously, Bayer, Belgium), mice were laid in a supine position on a thermopad at 37°C. The right common carotid artery was cannulated for blood sampling. The fur over the abdominal wall of the mice was shaved after meticulous disinfection with 70% alcohol. A silicon catheter (Venflon 22 G, 0.9 mm diameter, Terumo, Belgium) was inserted percutaneously into the right lower quadrant of the peritoneal cavity. This catheter was used for dialysate fluid infusion and sampling. Dialysate microsamples were taken from the bag at 0 minute, and from the Venflon catheter at 30 and 60 minutes, and at the end of the dwell (120 minutes). Prior to each sampling, 50 to 100 µL of the dialysate was flushed back and forth, and the abdomen was gently agitated to facilitate fluid mixing. Dialysate recovery was performed at the end of the dwell, using syringes and pre-weighed safe-lock tubes; the remaining dialysate in the peritoneal cavity was collected using gauze tissue (~5% of the recovered volume). Instilled and recovered dialysate volumes were weighed on a precision balance (AG35, Mettler Toledo; margin of error during experiments is 0.1 mg). Provided a dialysate density of 1.020 ± 0.001 g/cm³ in experimental conditions (3.86% glucose), the volume margin of error can be calculated as 0.1 µl. Values rounded of to 1 µl were used for both instilled and recovered volumes. These parameters were used to measure net UF, as previously described[5-6]. Previous experiments have demonstrated that a low intraperitoneal pressure in our mouse model of PD (<2 mmHg for IPV up to 10 ml) is

associated with a negligible absorption of fluid and fluorescently-labeled or radioiodinated albumin[4-6]; as a result, fluid absorption in basal conditions in our model can be neglected and net UF roughly represents transcapillary UF. Blood microsamples were taken from carotid artery at time 0, 30 and 60 minutes, and at the end of the dwell (exsanguination, 120 minutes). Hematocrit was measured before PD exchange. Plasma and dialysate urea and glucose, and plasma sodium were assayed using a Kodak Ektachem DT60 II and DTE II analyser (Eastman Kodak Company, USA). Dialysate sodium was determined using an indirect ion-selective electrode on a Roche Diagnostics Cobas 8000 Module ISE. Plasma and dialysate osmolality was measured using a Fiske Osmometer (Needham Heights, MA). Baseline characteristics of the animals are presented in Supplementary table 2. In some experiments, a single dose of lipopolysaccharide (10 mg/kg, *E. coli* serotype O111: B4; Sigma-Aldrich, Buchs, Switzerland) was instilled into the peritoneal cavity 24-h before assessing peritoneal transport.

Calculations. The transport of small solute was evaluated by the D/D_0 glucose ratio and the mass transfer area coefficient (MTAC) of urea, using (1) the Garred two-sample model[7] and (2) the Henderson and Nolph equation corrected for convective transport according to Waniewski[8]:

$$\text{MTAC urea (}\mu\text{L/min) (Garred)} = \frac{Vav}{t_{120}} \times \ln\left[\frac{V_0(P-D_0)}{V_t(P-D_t)}\right] \quad (1)$$

$$\text{MTAC urea (}\mu\text{L/min) (Waniewski)} = \frac{V_t}{t_{120}} \times \ln\left[\frac{V_0^{1-f}(P-D_0)}{V_t^{1-f}\ln(P-D_t}\right] \quad (2)$$

in which *Vav* is the average of the initial and final volumes; V_0, the instilled volume; V_t, the drained volume; *f*, a weighing factor between diffusion and convection (set at 0.33 for a large degree of convective transport, and at 0.5 for negligible convection); *P*, the plasma concentration of urea corrected for aqueous plasma water[9]; D_t, the dialysate concentration of urea at the end of the dwell; D_0, the initial concentration of urea in dialysate, which is set at 0. UF efficiency was calculated as the net UF (µL/g of body weight) divided by the amount of carbohydrates absorbed, as previously described[10].

Intraperitoneal volume vs. time curves. Intraperitoneal volume *versus* time curves were performed using a fluorescent bovine serum albumin conjugate as an indicator-dilution technique, as previously described[6], or by direct volumetry. Both techniques closely correlated, including when icodextrin was used as osmotic agent (Pearson *r*, 0.98, P=0.003). Dialysate sodium was measured using indirect ion selective electrode method.

Dynamic light scattering. Dynamic light scattering was used to determine the apparent hydrodynamic radius and size distribution profile of the glucose polymer icodextrin in solution (Extraneal 7.5%). The polydispersity index measurements were performed on a Malvern CGS3 equiped with a HeNe laser (λ=632.8 nm) at a temperature of 37.3°C and an angle of 90°. The size distributions were obtained by a CONTIN analysis of the data.

Determination of total icodextrin, icodextrin metabolites, and absorption of carbohydrates. Total icodextrin in the dialysate was measured by enzymatic hydrolysis with amyloglucosidase (Sigma-Aldrich, Saint-Louis, MO, USA); icodextrin metabolites were determined in the dialysate of mice exposed to 7.5% icodextrin using a weak anion-exchange column (BioBasic AX; 150 x 4.6 mm, 5 µm; Thermo Electron, Woburn, MA, USA) and a refractive index detector; and total HMW fractions were estimated as the difference between total icodextrin and LMW G2-G7 fractions, as previously described[11-14]. The amount of carbohydrates (CHO) absorbed from the peritoneal cavity was calculated as the difference between the mass of CHO (glucose and icodextrin) infused into the peritoneal cavity and the mass removed.

Mouse three-pore model. The mouse three-pore model is essentially the same as that used in the initial version[15] where LpS and other transport parameters have been adapted to the mouse based on separate experimental measurements of the osmotic conductance for glucose in *Aqp1*$^{+/+}$ and *Aqp1*$^{-/-}$ mice. The α_C parameter was set to 0.04 (i.e. slightly higher than in PD patients) to match the difference between *Aqp1*$^{+/+}$ and *Aqp1*$^{-/-}$ mice (using 3.86% glucose as the osmotic agent) and the osmotic water transport for icodextrin (which is essentially independent of σ_g and can therefore be used to estimate LpS). In their original version of the three-pore model, Rippe et al. had to inflate the mass transfer area coefficient for glucose to compensate for the fact that the rate of glucose disappearance from the peritoneal cavity was higher than that expected from the calculated rate of diffusion of glucose[15]. This correction was used unchanged in the present modelling studies. All relevant transport parameters were rescaled by $BW^{0.75}$ from man to mouse[16] and are shown in Table S1. The net flow of water to/from the mouse peritoneal cavity (equal to the change in the intraperitoneal volume V_D per unit time *t*) is described by the ordinary differential equation

$$\frac{dV_D}{dt} = J_{v,C} + J_{v,S} + J_{v,L} - L \qquad \text{(S1)}$$

where, $J_{v,C}$, $J_{v,S}$, and $J_{v,L}$ are the flows of water (in µL/min) across the aquaporins, the highly selective pathways (the "small pores") and the weakly selective pathways (the "large pores"),

respectively. L is the lymphatic flow (Table S1). The dialysate concentration for each solute *i* (denoted $dC_{D,i}/dt$ in mmol/L/min) as a function of time was calculated from

$$\frac{dC_{D,i}}{dt} = \frac{J_{s,S,i}+J_{s,L,i}}{V_D} - C_{D,i}\frac{J_{v,C}+J_{v,S}+J_{v,L}}{V_D} \quad \text{(S2)}$$

where $J_{s,S,i}$ and $J_{s,L,i}$ are the flows of solute i across the small pores and the large pores, respectively. The initial conditions are $V_D(0)$ = 2500 µL, $C_{D,glucose}(0)$ = see Table 1, $C_{D,Na+}(0)$ = 133 mmol/L for Icodextrin and 132 mmol/L for glucose fluids (Table 1), $C_{D,urea}(0)$ = 0 mmol/L, and $C_{D,albumin}(0)$ = 0. The initial concentrations for the icodextrin fractions were set according to Table S3. The initial value problem consisting of the ordinary differential equations S1 and S2 (one for each solute) and the initial conditions were solved with the Dormand-Prince (DOPRI) method[17]. The solute flow (in mmol/min) over each pathway is calculated according to the non-linear flux equation

$$J_{s,S,i} = J_{v,S}\left(1-\sigma_{s,i}\right)\frac{C_{P,i}-C_{D,i}e^{-Pe_{S,i}}}{1-e^{-Pe_{S,i}}} \quad \text{(S3)}$$

$$J_{s,L,i} = J_{v,L}(1-\sigma_{L,i})\frac{C_{P,i}-C_{D,i}e^{-Pe_{L,i}}}{1-e^{-Pe_{L,i}}} \quad \text{(S4)}$$

Here $C_{P,i}$ is the plasma concentration of solute *i* (set according to experimentally measured values); $\sigma_{S,i}$ and $\sigma_{L,i}$ the small- and large pore reflection coefficients (calculated from pore theory, see Eq. 4 in reference[15]); $Pe_{S,i}=J_{v,S}(1-\sigma_{S,i})/MTAC_{S,i}$ an $Pe_{L,i}=J_{v,L}(1-\sigma_{L,i})/MTAC_{L,i}$ are the Péclet numbers for the small and large pore pathway, respectively. The small- and large diffusion capacities, $MTAC_{S,i}$ and $MTAC_{L,i}$ (in µL/min), are either set according to Table S1 or calculated according to pore theory, see Eq. 11 in reference[15]. All reflection coefficients are calculated according to theory, see Eq. 4 in reference[15]. The flow of water across each pore population is calculated using

$$J_{vC} = \alpha_C L_p S\left(\Delta P - 19.3\sum_{i=1}^{N}\varphi_i\left(C_{P,i}-C_{D,i}\right)\right) \quad \text{(S5)}$$

$$J_{vS} = \alpha_S L_p S\left(\Delta P - 19.3\sum_{i=1}^{N}\varphi_i\sigma_{S,i}\left(C_{P,i}-C_{D,i}\right)\right) \quad \text{(S6)}$$

$$J_{vL} = \alpha_L L_p S\left(\Delta P - 19.3\sum_{i=1}^{N}\varphi_i\sigma_{L,i}\left(C_{P,i}-C_{D,i}\right)\right) \quad \text{(S7)}$$

Here α_C, α_S and α_L are the contributions for each of the different pathways to the barrier hydraulic conductance (see Table 1), φ_i is the osmotic coefficient of solute *i* set to 0.93 for sodium and related anions, cf. reference[15], and 1.0 for the other solutes. The hydraulic pressure gradient ΔP was set to 8 mmHg. Icodextrin fractions were the same as those used by

Rippe and Levin in their landmark publication, including trace amounts (~2 mmol/L) of glucose[15]. Additional simulations using the adapted version of the three-pore model showed that considering or not this negligible amount of glucose did not significantly impact net UF obtained with icodextrin (248 µl vs. 236 µl considering 8 icodextrin fractions or only the 7 fractions with a molecular weight >180 Da; <5% difference).

Estimation of icodextrin HMW distributions from DLS intensity data. The icodextrin molecules are relatively small compared to the wavelength of the incident light (λ=632.8 nm) and thus the intensity *I* of the scattered light can be estimated using the Rayleigh scattering equation

$$I = I_0 \frac{1+cos^2\theta}{2d^2}\left(\frac{4\pi^2 a_e^3}{\lambda^2}\right)^2\left(\frac{N^2-1}{N^2+2}\right)^2 \quad (1)$$

where I_0 is the incident light intensity; a_e the hydrodynamic radius of the solute, *d* the distance between the point of observation and the particle, *N* the particle to medium refractive index ratio and θ the angle between the incident and scattered light. Knowing the molecular weight MW and molecular density ρ of the solute, the above equation can be written

$$I = I_0 \frac{1+cos^2\theta}{2d^2}\frac{9\pi^2 MW^2}{\lambda^4\rho^2}\left(\frac{N^2-1}{N^2+2}\right)^2 \quad (2)$$

As a good approximation the molecular density ρ and refractive index for polymers are related via the well-known Lorenz–Lorentz relation $\rho = \frac{1}{r}\left(\frac{N^2-1}{N^2+2}\right)$ and thus, at a 90° angle of detection

$$I = I_0 \frac{9\pi^2}{2\lambda^4}\frac{r^2}{d^2}MW^2 \quad (3)$$

where *r* denotes the specific refraction (a tentative measure of properties like polymer shape and dipole strength) often assumed to be constant for a specific polymer-solvent system[18]. Moreover, the intensity of the scattered light is proportional to the molar concentration *n* yielding

$$I = \Lambda MW^2 n \quad (4)$$

where all the constants have been incorporated into Λ. Thus the parameter $\phi = \frac{I}{MW^2}$ is proportional to *n* and the fractional molarity *n%* of each fraction is π

$$n\% = \frac{I}{MW^2 \sum_K \phi} \quad (5)$$

where summation is performed over all fractions K. If the net molar concentration n_{net} is known then the molar concentration of each fraction is $n = n\% \cdot n_{net}$. The distribution of molecular weights of icodextrin was estimated using an empirical Mark-Houwink-Kuhn-Sakurada (MHKS) relationship

$$a_e = K'MW^{\varepsilon} \quad (6)$$

The MHKS-parameters K′ (0.486) and ε (0.385) were applied[15] and n_{net} was adjusted to give a mass concentration of 7.5%, 2.48% and 1.44% for un-fractionated and the two fractionated icodextrins, respectively. The scattered light intensity is proportional to the square of the solute molecular weight *vide infra* and DLS is therefore especially well suited to detect even minute amounts of high molecular weight solutes. For the same reason DLS data are inherently biased toward higher MWs, making LMW fractions undetectable in the current experiment. This effect was particularly evident for the unfractionated icodextrin solution but apparently less so for the fractionated solutions. LMW fractions were added in the TPM simulations (180 Da, 540 Da and 1 kDa fractions, identical to those used previously[15]) and, for unfractionated icodextrin, a 3 kDa fraction was added. Using the above procedure we obtained a number average M_n and mass average M_w for icodextrin of 6.3 kDa and 34.0 kDa, respectively, and a net molarity of 11.9 mmol/L (compared to ~12 mmol/L in reference[15]).

Statistical methods analysis. Data are presented as mean ± SEM. Comparisons between results from different groups were performed using *t* test, one- or two-way ANOVA, as appropriate. Significance level was indicated in the legend of each figure (**P*<0.05, ***P*<0.01, ****P*<0.001).

SUPPLEMENTARY FIGURES

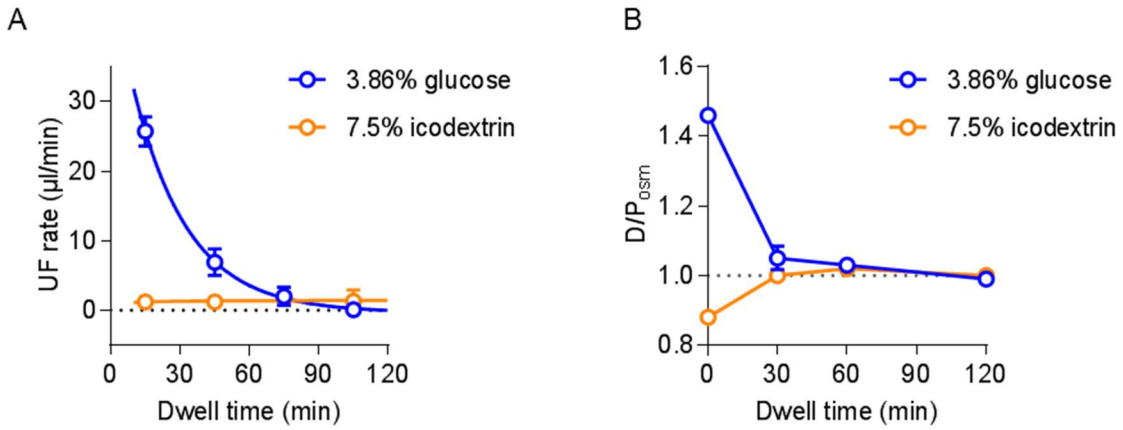

Supplementary Figure 1. Dynamic changes in UF rate and osmotic gradient using glucose or icodextrin in the mouse model of PD.

(A) Changes in UF rate and osmotic gradient over time using either 3.86% glucose (blue) or 7.5% icodextrin (orange) as osmotic agent in wild-type mice. (B) Changes in the osmotic gradient between the dialysate and plasma (D/P osmolality) over time on PD in wild-type mice, using hypertonic glucose (blue) or icodextrin (orange).

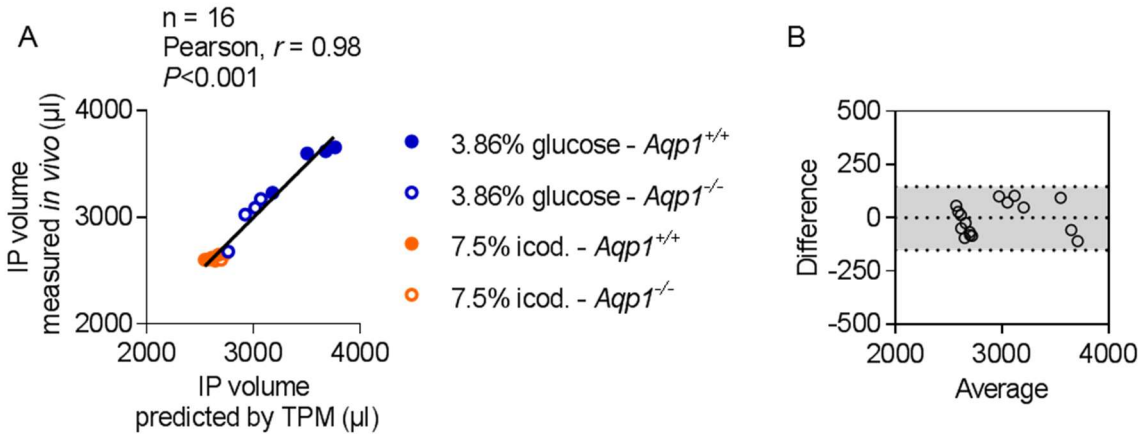

Supplementary Figure 2. Correlation and agreement between intraperitoneal (IP) volume measured *in vivo* and predicted by the three-pore model (TPM).

(A) Correlation line between IP volume measured by direct volumetry in the mouse model of PD and that predicted by computer simulations based on the TPM. (B) Bland-Altman analysis plot comparing both methods to assess IPV. Every circle represents the mean of IPV measured at 30, 60, 90 and 120 min of a dwell with either 3.86% glucose or 7.5% icodextrin in *Aqp1*$^{+/+}$or *Aqp1*$^{-/-}$ animals. Dotted lines in the Bland-Altman graph represent mean ± 95% limits of agreement. Bias (±SD) was -3.6 (±76.0), and 95% limits of agreement, -152.5 to 145.4.

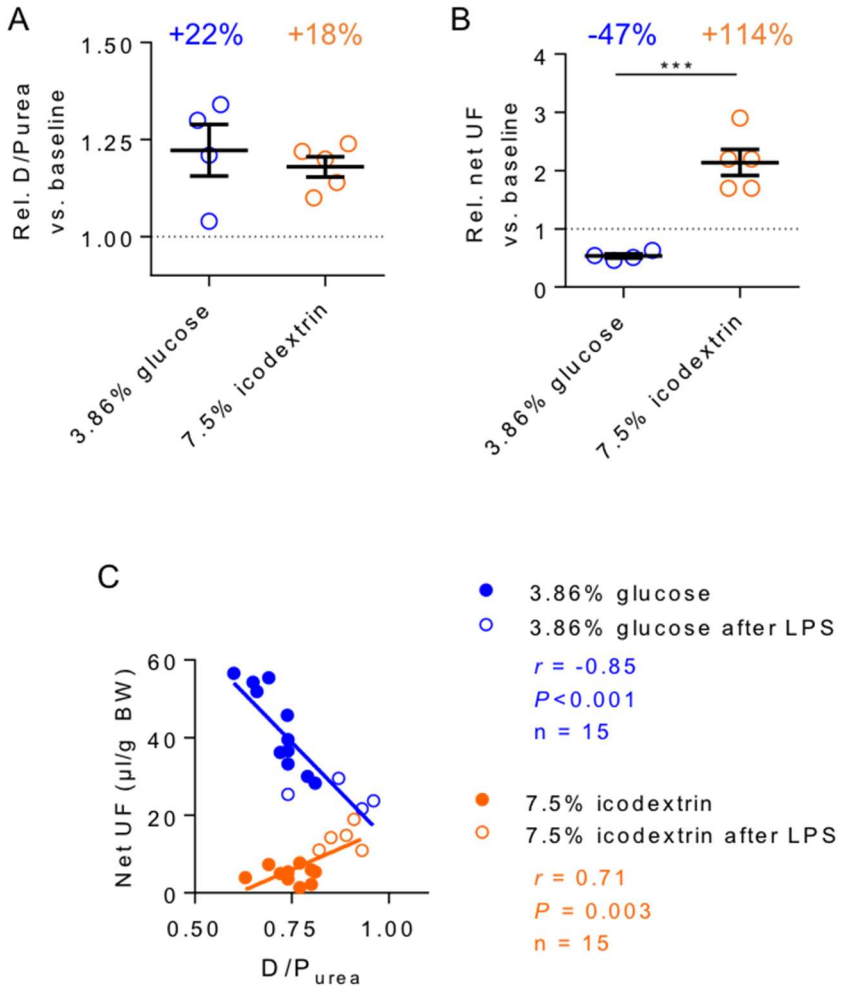

Supplementary Figure 3. Effect of lipopolysaccharide-induced modulation of peritoneal solute transport on water removal achieved by hypertonic glucose vs. icodextrin in the mouse model of PD.

(A) Relative dialysate-over-plasma (D/P) urea ratio 24-h after exposure to intraperitoneal (IP) lipopolysaccharide (LPS), during dialysis with either 3.86% glucose (blue circles) or 7.5% icodextrin (orange circles). (B) Relative net ultrafiltration (UF) at the end of 2-h dwells in the same animals. (C) Relationship between net UF and solute transport using either hypertonic glucose (blue) or icodextrin (orange), in basal conditions (closed circles) and after LPS exposure (open circles). Data are mean ± SEM; each circle represents a mouse.

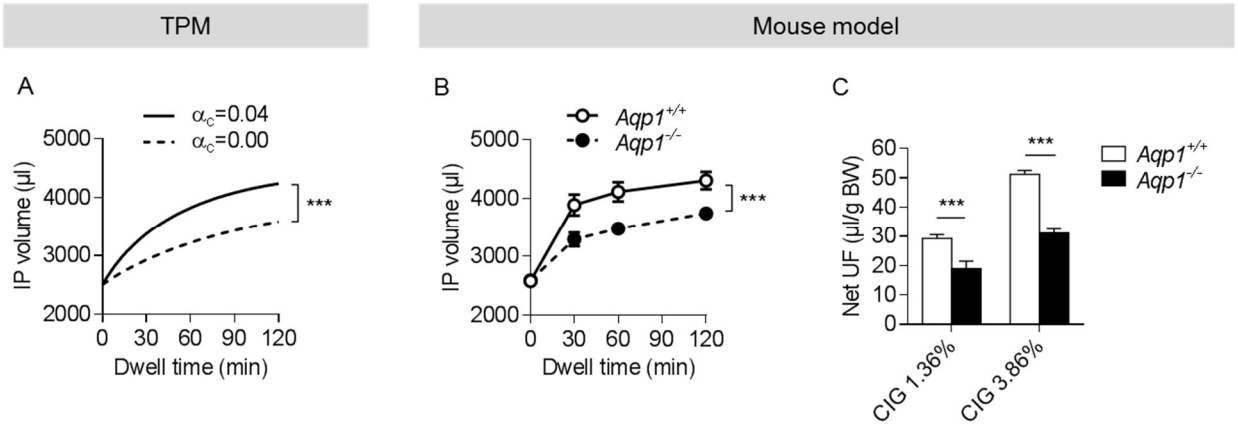

Supplementary Figure 4. Role of AQP1 in osmotic water transport induced by combinations of icodextrin and glucose.

(A) Predictions from the three-pore model (TPM) showing the changes in the intraperitoneal (IP) volume over time during P with a combination of icodextrin and glucose (CIG) 3.86%, using a fractional ultrafiltration coefficient for ultrasmall pores of 0.04 (solid line) or 0.00 (dotted line), respectively. (B) Changes in IP volume over time during PD with CIG 3.86% in *Aqp1* wild-type (open circles, solid line) *vs.* knockout (close circles, dotted line) mice. (C) Net ultrafiltration (UF) at the end of 2-h dwells with CIG 1.36% or CIG 3.86% in *Aqp1* mice. Data are mean ± SEM; n = 4-6/group.

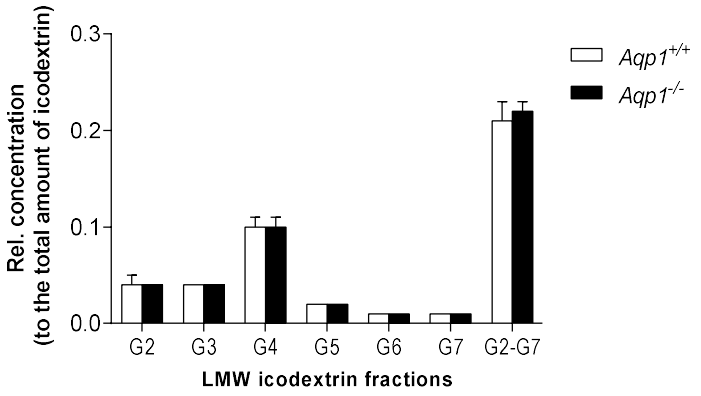

Supplementary Figure 5. Relative concentration of low molecular weight icodextrin metabolites (G2-G7) to the total icodextrin concentration in the peritoneal effluent of *Aqp1* mice.

At the end of a 2-h dwell with 7.5% icodextrin, smaller low molecular weight icodextrin metabolites (G2-G4) predominate over the larger ones (G5-G7), suggesting intraperitoneal metabolism of the glucose polymers. No difference is observed between *Aqp1*$^{+/+}$ and *Aqp1*$^{-/-}$ mice. Data are mean ± SEM; n=6 in each group.

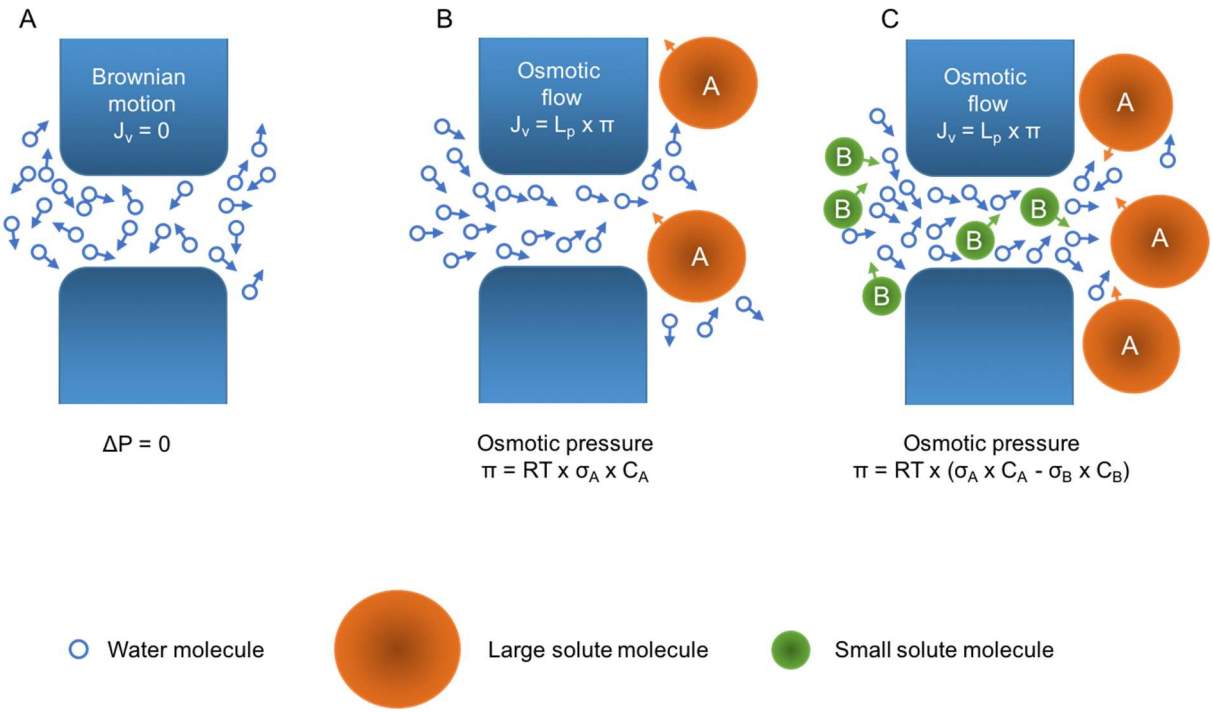

Supplementary Figure 6. Molecular mechanisms of osmosis.

(A) Brownian motion of water molecules through a membrane pore with water on both sides. The amount of water molecules that diffuses in the two directions is balanced so precisely that zero net movement of water occurs. (B) Osmotic flow through a water filled membrane pore from the water side towards a dilute solution containing large, near impermeable, solute molecules in a concentration C_A. Osmotic water flow will continue until the solute concentration becomes equal on both sides of the membrane. The osmotic pressure exerted by particles in solution is determined by the number of particles per unit volume of fluid and their reflection coefficients, not by the mass of the particles. (C) Osmotic flow between solutions of equimolar concentration (isotonic flow). Although the concentrations are equal, osmotic flow proceeds from left to right because the reflection coefficient (σ) for solute A is larger than for solute B. From a conceptual point of view, situation B is like the osmotic water flow at the level of solute-impermeable water-only channels (transcellular route, ultrasmall pores). On the contrary, situation C may reflect water transport across interendothelial clefts (paracellular route, small pores). Hydrostatic pressure is considered equal on both sides of the membrane in all three situations. J_v, osmotic water flow; L_p, conductance; R, gas constant; T, absolute temperature. Adapted from reference[19].

SUPPLEMENTARY TABLES

Supplementary Table 1. Parameters of the modified, mouse-adapted three-pore model.

	Aqp1$^{+/+}$	*Aqp1*$^{-/-}$
Transperitoneal hydrostatic pressure gradient (ΔP) - mmHg	8	8
Transperitoneal oncotic pressure gradient (Δπ) - mmHg	22	22
Unrestricted pore area over unit diffusion distance ($A_0/\Delta x$) - cm	70	70
MTAC for glucose - µL/min	30	30
MTAC for sodium - µL/min	20	20
MTAC for urea - µL/min	50	50
UF coefficient (LpS) - µl/min/mmHg	0.15	0.12
Osmotic conductance to glucose (LpS σ_g) – nl/min/mmHg	10	3.5
Peritoneal lymph flow (L) - µl/min	0.8	0.8
Fractional LpS small pores (α_s)	0.88	0.92
Fractional LpS ultrasmall pores (α_c)	0.04	0.00
Fractional LpS large pores (α_L)	0.08	0.08

MTAC, mass transfer area coefficient; UF, ultrafiltration

Supplementary Table 2. Clinical and biological characteristics of *Aqp1* mice at baseline.

Solution	Groups	Body weight (g)	Hematocrit (%)	Plasma sodium (mmol/L)
1.36% glucose	*Aqp1*$^{+/+}$	27.2±0.8	48.8±0.3	143.8±0.5
	Aqp1$^{-/-}$	26.4±0.9	48.5±0.6	144.8±1.6
3.86% glucose	*Aqp1*$^{+/+}$	26.8±0.5	48.0±0.5	144.5±0.6
	Aqp1$^{-/-}$	24.7±0.6	47.3±0.5	147.7±0.8
1.1% aminoacids	*Aqp1*$^{+/+}$	26.1±0.7	50.2±0.8	144.0±1.5
	Aqp1$^{-/-}$	25.4±1.3	48.5±0.6	146.8±1.3
7.5% icodextrin	*Aqp1*$^{+/+}$	24.8±0.7	49.8±0.9	144.2±1.1
	Aqp1$^{-/-}$	25.2±1.0	50.5±1.0	141.2±1.9

REFERENCES

1. Ma T, Yang B, Gillespie A, Carlson EJ, Epstein CJ, Verkman AS. Severely impaired urinary concentrating ability in transgenic mice lacking aquaporin-1 water channels. *J Biol Chem* 273:4296-4299, 1998
2. Ni J, Moulin P, Gianello P, Feron O, Balligand JL, Devuyst O. Mice that lack endothelial nitric oxide synthase are protected against functional and structural modifications induced by acute peritonitis. *J Am Soc Nephrol* 14:3205-3216, 2003
3. Ni J, Cnops Y, Debaix H, Boisdé I, Verbavatz JM, Devuyst O. Functional and molecular characterization of a peritoneal dialysis model in the C57BL/6J mouse. *Kidney Int* 67:2021-2031, 2005
4. Ni J, Verbavatz JM, Rippe A, Boisdé I, Moulin P, Rippe B, Verkman AS, Devuyst O. Aquaporin-1 plays an essential role in water permeability and ultrafiltration during peritoneal dialysis. *Kidney Int* 69:1518-1525, 2006
5. Yool AJ, Morelle J, Cnops Y, Verbavatz JM, Campbell EM, Beckett EA, Booker GW, Flynn G, Devuyst O. AqF026 is a pharmacologic agonist of the water channel aquaporin-1. *J Am Soc Nephrol* 24:1045-52, 2013
6. Morelle J, Sow A, Vertommen D, Jamar F, Rippe B, Devuyst O. Quantification of osmotic water transport *in vivo* using fluorescent albumin. *Am J Physiol Renal Physiol* 307:F981–9, 2014
7. Garred LJ, Canaud B, Farrell PC. A simple kinetic model for assessing peritoneal mass transfer in chronic ambulatory peritoneal dialysis. *ASAIO J* 6:131–137, 1983
8. Waniewski J, Werynski A, Heimbürger O, Lindholm B. Simple models for description of small solute transport in peritoneal dialysis. *Blood Purif* 9:129–141, 1991
9. Waniewski J, Heimbürger O, Werynski A, Lindholm B. Aqueous solute concentrations and evaluation of mass transport coefficients in peritoneal dialysis. *Nephrol Dial Transplant* 7:50-56, 1992
10. Holmes C, Mujais S. Glucose sparing in peritoneal dialysis: implications and metrics. *Kidney Int* 103:S104-9, 2006
11. García-López E, Pawlaczyk K, Anderstam B, Qureshi AR, Kuzlan-Pawlaczyk M, Heimbürger O, Werynski A, Lindholm B. Icodextrin metabolism and alpha-amylase activity in nonuremic rats undergoing chronic peritoneal dialysis. *Perit Dial Int* 27:415-423, 2007
12. García-López E, Werynski A, Heimbürger O, Filho JC, Lindholm B, Anderstam B. Rate of synthetic oligosaccharide degradation as a novel measure of amylase activity in peritoneal dialysis patients. *Perit Dial Int* 28:296-304, 2008
13. Davies SJ, Garcia Lopez E, Woodrow G, Donovan K, Plum J, Williams P, Johansson AC, Bosselmann HP, Heimburger O, Simonsen O, Davenport A, Lindholm B, Tranaeus A, Divino Filho JC. Longitudinal relationships between fluid status, inflammation, urine volume and plasma metabolites of icodextrin in patients

randomized to glucose or icodextrin for the long exchange. *Nephrol Dial Transplant* 23:2982-8, 2008

14. García-López E, Lindholm B. Icodextrin metabolites in peritoneal dialysis. *Perit Dial Int* 29:370-6, 2009
15. Rippe B, Levin L. Computer simulations of ultrafiltration profiles for an icodextrin-based peritoneal fluid in CAPD. *Kidney Int* 57:2546-2456, 2000
16. Singer MA, Morton AR. Mouse to elephant: biological scaling and Kt/V. *Am J Kidney Dis* 35:306-9, 2000
17. Dormand JR, Prince PJ. A family of embedded Runge-Kutta formulae. *J Comput Appl Math* 6:19-26, 1980
18. Georgalis Y, Philipp M, Leksandrova R, Krüger JK. Light scattering studies on Ficoll PM70 solutions reveal two distinct diffusive modes. *J Colloid Interface Sci* 386:141–147, 2012
19. Kiil F. Mechanism of osmosis. *Kidney Int* 21:303-8, 1982